Article

Overview of Nano-fiber Bundles Fabrication via Electrospinning and Morphology Analysis

Amirhossein Ahmadian [1,*], Abbas Shafiee [2,4,*], Nojan Aliahmad [3], and Mangilal Agarwal [4]

[1] Department of Mechanical and Aerospace Engineering, University of California, Los Angeles, CA, 90095, USA; aahmadian@ucla.edu
[2] School of Mechanical Engineering, Purdue University, West Lafayette, IN, 47907, USA; shafiee@purdue.edu
[3] School of Electrical Computer Engineering, Purdue University, West Lafayette, IN, 47907, USA; naliahma@purdue.edu
[4] Department of Mechanical and Energy Engineering, Indiana University-Purdue University Indianapolis, Indianapolis, IN, 46202, USA; agarwal@iupui.edu; ashafie@iu.edu
[5] Integrated Nanosystems Development Institute, Indiana University-Purdue University Indianapolis, Indianapolis, IN, 46202, USA
* Correspondence: aahmadian@ucla.edu; shafiee@purdue.edu

Abstract: Electro-spun ultra-fine fibers exhibit two significant properties: a high surface-to-volume ratio and a relatively defect-free molecular structure. Due to the high surface-to-volume ratio, electro-spun materials are well suited for activities requiring increased physical contact, such as providing a site for a chemical reaction or filtration of small-sized physical materials. However, electrospinning has many shortcomings, including difficulties in producing inorganic nanofibers and a limited number or variety of polymers used in the process. The fabrication of nanofiber bundles via electrospinning is explored in this analytical study, as well as the relationship between extrinsic electrospinning parameters and the relative abundance of various fiber morphologies. Numerous variables could impact the fabrication of nanofibers, resulting in a variety of morphologies; therefore, adequate ambient conditions and selecting the appropriate solvent for achieving a homogenous polymer solution and uniform electro-spun materials are examined. Finally, common polymers suitable for electrospinning and the promising applications of ultra-fine fibers achieved via electrospinning are studied in this paper.

Keywords: Electrospinning; Nano-fiber; Morphology

1. Review on Electrospinning and Electrostatic Phenomenon

Formhals invented electrospinning as a fiber spinning technique in the early 1930s. The invention, named "method and apparatus for preparing artificial threads," was patented in 1934 and advanced spinning techniques. However, some practical problems persisted, such as fiber drying and collection, until he filed his first patent, which addressed spinning difficulties at the time. A movable thread was used to collect the stretched threads. He explained the spinning of cellulose acetate fibers using acetone as the solvent in his patent [1,2].

Electrostatic phenomena are induced by electrons' relative ease of movement in different materials. Electrostatics is classified into two broad categories: conduction and induction. Induction is a transient state of matter in which electrons are either drawn to or repelled by a neighboring charged material. [3]. On the other side, conduction occurs when a charged object establishes physical contact with a neutral object. When excess electrons are transferred from a charged object to a neutral object, the objects gain the same charge [4]. Electrostatic charges exert forces calculated using Coulomb's law $F = k\, Q1.Q2/d^2$ between opposite charges causing water droplet deformation [5]. Electrospinning is a general term that refers to the process of producing fibers by the use of an electric current to draw charged threads of polymer solutions. Typically, the fibers produced by this process have a thickness of hundreds of nanometers. Electrospinning is a method that combines the characteristics of dry spinning and electrospraying of fiber [6]. The method is ideal for the

check for updates

Citation: Ahmadian, A. Title. *Preprints* **2021**, *1*, 0. https://doi.org/

Received:
Accepted:
Published:

Preprints (www.preprints.org) | NOT PEER-REVIEWED | Posted: 27 April 2021 doi:10.20944/preprints202104.0711.v1

processing of complex and large molecules because it does not require the use of chemistry coagulation or high temperatures [7–12].

2. Overview of Nano-fiber Bundles Fabrication Methods and Electro-spinning

Nanofibers are fibers with a diameter less than 1000nm; they can be created through a variety of processing techniques [7,8]. So far the nano-fiber making techniques include direct drawing [13–15], magneto-spinning [16], extrusion [17,18], melt-blowing [19], hard templating [20], soft-templating [21], self-assembly [21,22], lithography [23,24], centrifuge spinning [25,26], hydrothermal/solvothermal [27], ball milling [28], chemical vapor deposition [29,30], and electrospinning [31–34]. Among them, electrospinning outperforms due to its numerous advantages, including controllable fiber diameter (from tens of nanometers to a few microns), ability to fabricate a wide variety of materials (natural and synthetic polymers, metals, ceramics, composites, and sol-gels), and a variety of fiber morphologies (porous, dense, core-sheath, hollow, spiral, side-by-side, nanoparticles, nanorods, nanowires, nanosheets, and nanobelts), and capable of large scale production [7–11].

The formation of nanofibers is a function of the electrostatic force acting in conjunction with the spinning force, resulting in the continuous splitting of polymer droplets. Nanofibers deposit layer upon layer on the metal collector plate, resulting in the formation of a nanofibrous mat [35–37].The extrinsic parameters of the electrospinning process have an important effect on the structural morphology of the nanofibers. The working distance, viscosity, conductivity, polymer solution, humidity, and temperature, as well as the applied voltage, are all extrinsic parameters. It is important to optimize the extrinsic parameters in order to obtain a uniform nanofiber mat. When the nano-fibrous mat is uniform, it forms a fibrous structure with beads and a continuous fibrous structure (nanofiber yarns). Nanofiber yarns are classified as entangled continuous fiber bundles that exhibit two inherent characteristics: continuous length and a twisted structure that is interlocked [38].

Correlations between extrinsic electrospinning parameters and the relative abundance of various fiber morphologies result in the formation of various nanofiber bundle structures. [39]. In general, nanofiber bundles can be categorized as seen in the following [40] (See Figure 1):

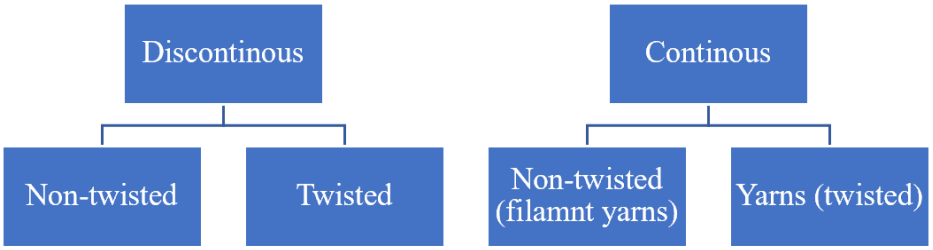

Figure 1. Nanofiber bundle categories.

3. Electrospinning Categories

Electrospinning could be used to produce nanofibers in two ways: needle-free or needle-based. Needle-based electrospinning begins with a polymer solution contained in a tightly sealed tank, which both restricts and prevents solvent evaporation. The needle-based method is critical because it enables the handling of a wide variety of materials, including those that are extremely volatile [41]. Needle-based electrospinning offers the following advantages: process versatility, including the ability to process fibers with multi-axial and core-shell structures. The distinction between the two fibers allows the fiber to integrate Active Pharmaceutical Ingredients (API). Additionally, the needle-based approach allows for precise monitoring of the flow rate, minimizes solution waste, and utilizes a

Preprints (www.preprints.org) | NOT PEER-REVIEWED | Posted: 27 April 2021 doi:10.20944/preprints202104.0711.v1

small number of jets. Numerous benefits have contributed to the needle-based method's widespread usage [42].

On the other side, needle-free electrospinning enables large-scale material processing. Using a rotating or stationary base, a starting polymer solution is used to produce nanofibers [43]. The needle-free electrospinning process, on the other hand, is incapable of producing diverse fibers. Additionally, numerous process variables, including the flow rate, cannot be controlled [44].

4. Electrospinning Process and Principles

Electrospinning is a method that uses submicron fiber to create an impermeable nonwoven fabric by forcing a liquid jet with a millimeter diameter through an electric field-induced nozzle. In general, the electrospinning fiber forming process can be observed and split into 3 distinct stages: prolate droplet deformation (Taylor cone) and jet initiation, whipping or bending instability, and fiber deposition. The general setup for electrospinning is shown in Figure 2. The electrostatic charge at the nozzle's tip is critical for the creation of a Taylor cone at the point of ejection of a single jet of fluid [36]. The electric field's acceleration and thinning of the jet, combined with radial charge repulsion, cause the primary jet to break into several filaments; this phenomenon is referred to as "splaying." The diameter of the resulting fibers is determined by the number of subsidary jets produced. Under normal conditions, electrospinning's fluid jet whipping is relatively fast, which is necessary for the development of nanofibers [45].

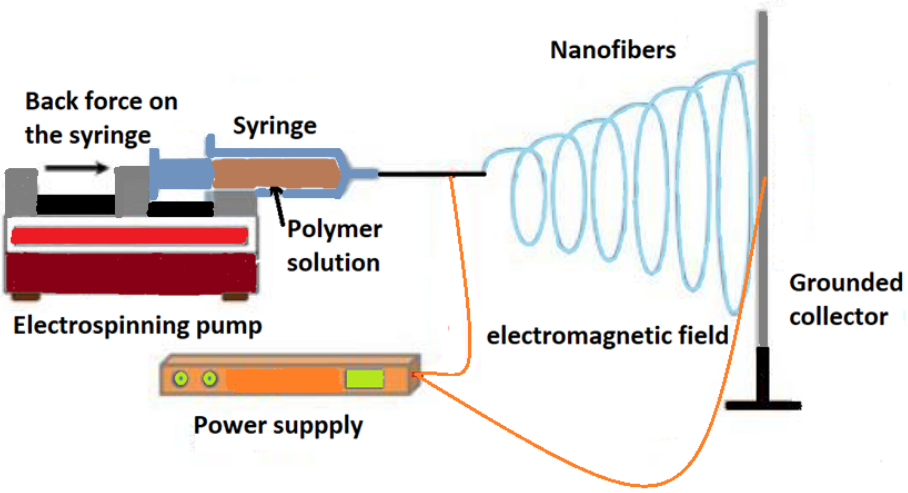

Figure 2. General electrospinning setup.

In general, the fiber formation process in electrospinning can be observed and classified into three different stages: Deformation of the prolate droplet (Taylor cone) and jet initiation, whipping or bending instability, and fiber deposition.

4.1. Taylor Cone

Geoffrey Taylor first identified the cone in 1964. Taylor was primarily interested in the behavior of water droplets in the presence of intense electric fields, such as those found in thunderstorms. When a small volume of an electrically conductive liquid is exposed to an electric field, the form of the liquid is distorted due to surface tension. Voltage increases the effect of the electric field, and because the electric field exerts a magnitude force on the droplet comparable to the surface tension, a cone shape forms. When a predetermined threshold voltage is reached, the rounded tip inverts and then releases a jet of liquid. The

Preprints (www.preprints.org) | NOT PEER-REVIEWED | Posted: 27 April 2021 doi:10.20944/preprints202104.0711.v1

cone-jet initiates the electrospraying process when the voltage exceeds the threshold. The Taylor cone denotes the theoretical limit of a cone-jet at the start of the electrospraying operation. To achieve a perfect cone, a semi-vertical angle of 49.3 degrees must exist, the cone surface must be equipotential, and the cone must exist in steady-state equilibrium [46]. The formation of Taylor cone is a critical step in the electrospinning process. The formation of symmetrical vortices within the Taylor cone is likely to increase the solution's velocity. Cone-jet beads result in the formation of beaded nanofibers [47].

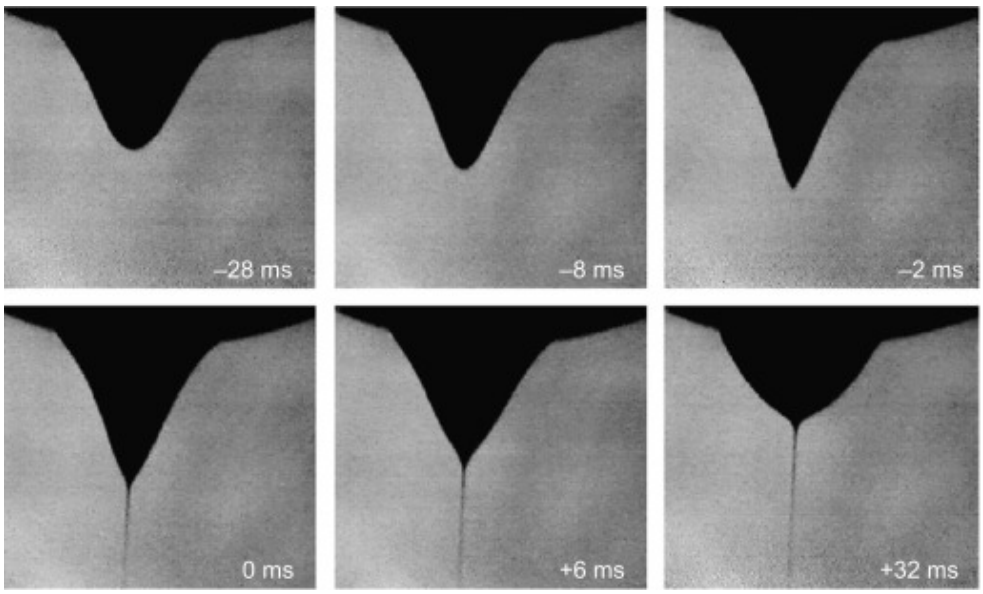

Figure 3. By increasing the electric field, deformations of the prolate droplet and Taylor cone are captured at various times (-28ms, -8ms, -2ms, 0 ms, +6ms, and +32ms), culminating in the formation of the jet [37].

In Figure 3, the formation of a Taylor cone captured in different timings can be observed.

4.2. Whipping and Jet Instability

A strong electric field could deform a liquid with a finite electric conductivity into a conical shape due to the balance of surface tension and electric stresses. In contrast, at the cone's apex, the structure becomes unstable, and the resulting singularity is replaced by the thin jet structure. The electrospray is caused by the forced flow rate of the liquid inside the cone-jet structure, which is stable at certain applied voltage values — the electrospray is caused by the cone-jet structure collapsing into spherical droplets as a result of axisymmetric instabilities. However, due to electrostatic repulsion between the straight and bent sections of the jet, a lateral instability causes the jet to bend off its axis. When the whipping instability growth rate exceeds that of a jet breakup, the jet's off-axis movement becomes a significant part of its evolution [48].

By substituting a polymer solution for a liquid and allowing the solvent to evaporate prior to drop breakup, polymer fibers are formed. The presence of lateral instability in the electrospinning process results in the creation of thinner fibers as the bending proceeds to stretch and thins the jet. However, in the majority of experiments, the whipping is notably chaotic, rendering an in-depth understanding of its properties and structure challenging [7,8,48].

4.3. Fiber Deposition

The formation of nanofibers is induced by an electrostatic force combined with a spinning mechanical force, which results in the continuous splitting of polymer droplets.

Preprints (www.preprints.org) | NOT PEER-REVIEWED | Posted: 27 April 2021 doi:10.20944/preprints202104.0711.v1

Nanofibers deposit layer upon layer on the metal collector plate, resulting in the formation of a nanofibrous mat [35–37].

5. Solution-based Electrospinning and Related Effective Parameters

Electrospinning using a solution requires a solvent to solubilize the polymer. As a result, selecting the appropriate solvent is critical for achieving a homogeneous polymer solution. The solution parameter is advantageous in deciding a solvent that is ideal for a particular polymer. The solubility parameter takes into account all of the molecular interactions that occur within a given mole of material, including polar interactions, dispersion forces, and basic interactions such as hydrogen bonding. [49]. Cohesive energy is given as

$$E = \Delta H - RT \tag{1}$$

Where: ΔH is Latent heat of vaporization, T is Absolute temperature, and R is Universal gas constant.
Later, Charles M. Hansen extended Hildebrand's theory of solubility to Hansen Solubility Parameters (HSP) 21, which quantifies the relative miscibility of polar and hydrogen bonding systems as [50]:

$$\delta_i{}^2 = \delta_d{}^2 + \delta_p{}^2 + \delta_h{}^2 \tag{2}$$

where: δ_i is Hansen solubility parameter, δ_d is Dispersive component, δ_p is the polarity, and δ_h is the hydrogen bonding. A solvent that is suitable for a particular polymer should have a solubility parameter that is similar to that of the polymer. As a result, when calculating the Hansen solubility parameter, the polymer-solvent should have a low value of Ra [51].

$$Ra^2 = 4(\delta_{d1} - \delta_{d2})^2 + (\delta_{p1} - \delta_{p2})^2 + (\delta_{h1} - \delta_{h2})^2 \tag{3}$$

Additionally, a suitable solvent ought to have a relative energy difference (RED) of less than one. And RED = Ra/Ro Where Ro refers to the radius of a sphere [51]. where: RED < 1 the molecules are similar and dissolve, RED = 1 the molecules partially dissolve, and RED > 1 the molecules do not dissolve.

Numerous variables can impact the fabrication of nanofibers, resulting in a variety of morphologies such as a uniform or ordered pattern structure with a round cross-section, beads-on-string structures, or individual beads. These critical factors include the type of polymer, the molecular weight of the polymer, the distribution of the polymer, and the concentration of the polymer [52,53], solution conductivity, solution surface tension, solution viscosity, and solvent properties. Solvent properties contain boiling point, volatility, and dielectric properties [54]. Another critical parameters affecting the final fiber morphology are indeed the applied voltage, collecting distance, and polymer solution flow rate [55]. Finally, external conditions or ambient conditions such as high humidity, ambient temperature, and addition flow are all effective factors to be taken in to account for electrospinning [7,8,33,56].

5.1. Concentration

The electrospinning process is highly dependent on the polymer concentration. As a result, changing the polymer concentration results in a change in the viscosity of the solution. As the polymer concentration increases, the viscosity increases gradually at first and then rapidly [57]. Within a polymer solution, the viscosity is largely determined by intermolecular interactions between polymer and polymer, polymer and solvent, and solvent-solvent. Similar to electrospraying, electrospinning a dilute polymer solution is analogous to electrospraying. On the other hand, the intermolecular distance between polymers within a solution is so considerable so that the interaction is considered to be quite weak. As a result, the viscoelastic force in the polymer jet is negligible, allowing for the formation of a uniform fibrous structure. As the voltage is applied, the jet splits into separate charged sections. As a result of the high surface tension caused by solvent evaporation during spinning, these charged sections gradually transform into droplets

Preprints (www.preprints.org) | NOT PEER-REVIEWED | Posted: 27 April 2021 doi:10.20944/preprints202104.0711.v1

or individual beads (see Figure 4. Similarly, increasing the polymer concentration results in a greater viscoelastic force and makes splitting the jet more difficult. Rather than dissolving the like-charged sections, electrostatic repulsion within the solution elongates the connections between charged sections, resulting in thinner filaments. Although the links between charged sections are thinner, the sections that are relatively thicker stretch thinner. Due to the surface tension created as the solvent evaporates during spinning, filaments tend to take on the shape of beads-on-string morphology (see Figure 5). As a result, increasing the polymer concentration results in uniform jet elongation and formation, resulting in a homogeneous and uniform fiber morphology (see Figure 6)[7,8,57,58].

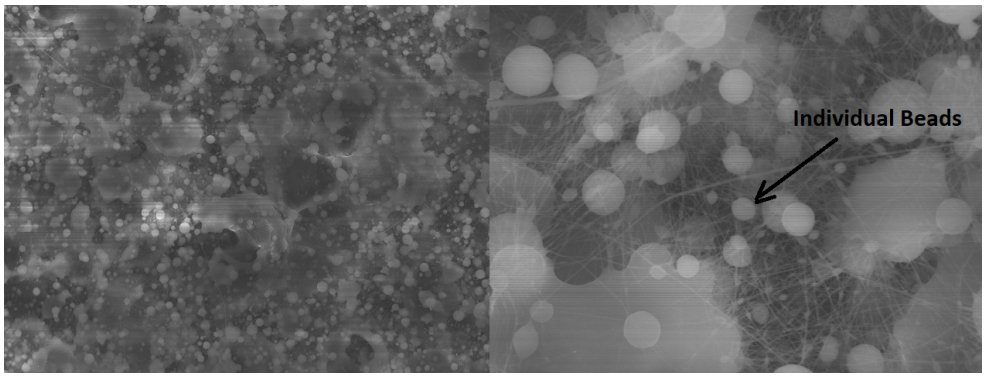

Figure 4. An example of individual beads textile resulted from polymerized electro-spun V_2O_5 with PVP diluted in water [59].

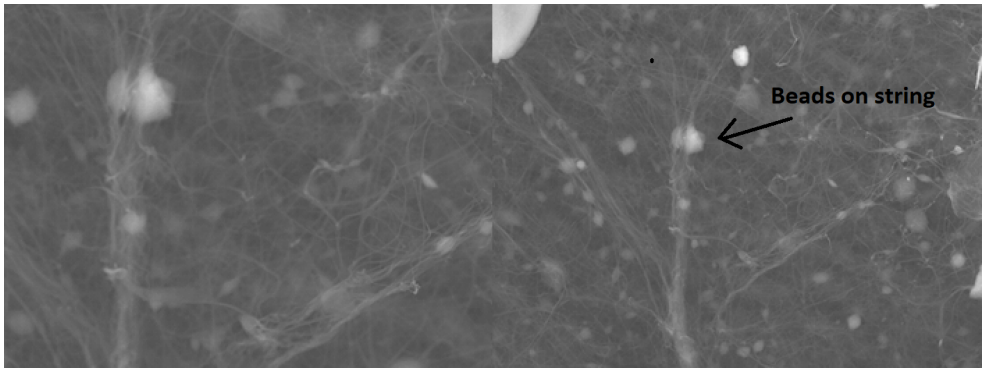

Figure 5. An example of beads on strings of textile resulted from polymerized electro-spun V_2O_5 with PVP diluted in water [59].

The critical concentration (c*) is used to determine whether or not there will be significant intermolecular interaction, resulting in chain entanglement. [60]. The following formula has been used to describe solution entanglement in this context. The following formula determines the ratio of the molecular weight of the polymer to the molecular weight of the solution entanglement [61,62]:

$$(n_e)_{solution} = \frac{M_W}{(M_e)_{solution}} = \frac{\phi M_W}{M_e} \tag{4}$$

where: M_e is entanglement molecular weight, M_W is polymer weight average molecular weight, and ϕ is polymer volume fraction.
if $(n_e)_{solution} < 2$: polymer chains do not entangle and individual beads structure is formed.
if $2 < (n_e)_{solution} < 3.5$: insufficient polymer chain entanglement and beads-on-string structure is resulted.
if $(n_e)_{solution} > 3.5$: sufficient polymer chain entanglement and beads-on-string structure is

Preprints (www.preprints.org) | NOT PEER-REVIEWED | Posted: 27 April 2021 doi:10.20944/preprints202104.0711.v1

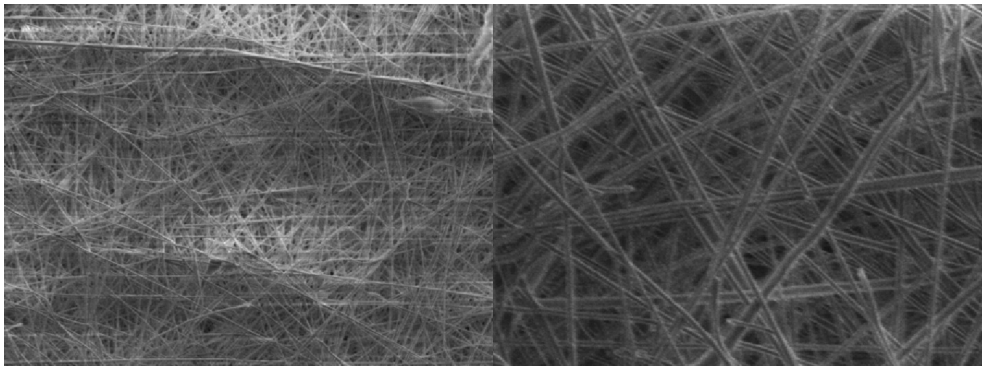

Figure 6. An example of uniform textile resulted from polymerized electro-spun V_2O_5 with PVP diluted in water [59].

shaped.

In general, the solution viscosity can be increased during electrospinning by either using a concentrated polymer solution or by increasing the molecular polymer's weight. For example, doping polylactide solutions with high-molecular-weight polyethylene oxide increases the viscosity of polymer solutions [63]. Increased viscosity improves the jet stability, enabling the construction of multifilament yarns, individual fibers, and unidirectionally aligned fibers across a large area, or allowing the individual filaments to develop an ordered pattern [64].According to literature, using polymers with a higher molecular weight and increasing the viscosity of the electrospinning solution results in a more stable jet [56].

5.2. Solvent

The process of electrospinning is highly dependent on the solvent selection. Because the conductivity, viscosity, and surface tension of a solution are influenced by a number of solvent properties, such as conductivity, boiling point, vapor pressure, polarity, dipole moment, and dielectric constant. The volatility of the solvent should be proportional to the travel time of the jet, i.e., low volatility solvents result in a wet web structure. Similarly, rapid evaporation of highly volatile solvents causes the filament surface to cool and freeze, resulting in a porous surface on the web structure [65] (see Figure 7).

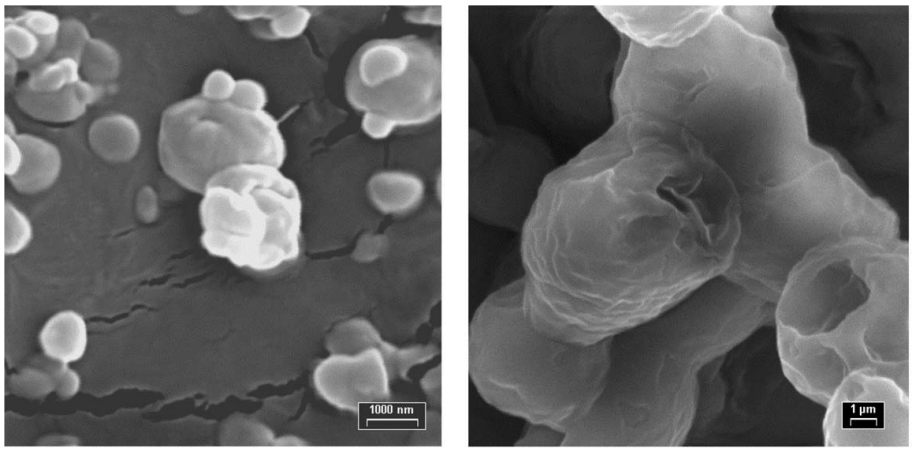

(a) (b)

Figure 7. (a) solid beads vs.(b) porous beads produced by electrospinning [65].

A solution's electrospinnability can be increased by doping it with salt or by using a solvent with a high dielectric constant and conductivity, which increases the spinning jet charge density. However, these same factors result in a shorter length jet, which should be avoided if the primary objective is to acquire a stable jet of greater length. Doping

Preprints (www.preprints.org) | NOT PEER-REVIEWED | Posted: 27 April 2021 doi:10.20944/preprints202104.0711.v1

polyethylene oxide with salt results in increased conductivity and a shorter stable jet. However, the critical conductivity between the bending instability and the long stable jet is estimated to be as low as 0.6 $\mu S/cm$ in the chloroform system [66].

5.3. Voltage and Electric Field

Traditionally, an increase in voltage results in an increase in the length of a stable jet during the electrospinning process. The increased length is the result of a stronger tangential electric field generated at the needle tip and a lower static charge density used to stabilize the electrospinning jet. The conventional effect, on the other hand, does not apply to all solutions. The inconsistency could be caused by a variety of factors, including the solution's dielectric property and conductivity. These variables have a greater impact on jet stability [67].

The applied voltage has an effect on the jet's bending and stretching stability, as a uniformly patterned web may result in some cases at higher voltages. However, the applied voltage is not the only critical factor to consider; other factors such as flow rate, jet traveling speed, and density must also be considered [68].

Typically, the electrospinning process utilizes direct-current (DC) voltage; however, alternating-current (AC) voltage has been reported in a few papers and is not considered as safe as DC voltage, especially in high voltage situations [69–71]. When highly aligned fibers are desired, the reason for utilizing AC could be witnessed. When an alternating current power source is applied, a highly aligned web structure is gathered on a rotating mandrel [72].

5.4. Flow Rate

The solution flow rate must be reduced to a minimum point where the spinning jet can compensate for solution evaporation in order to maintain continuous fiber flow [73]. If the flow rate is higher than required, solution will accumulate at the tip of the needle, preventing the formation of a normal Taylor cone and eventually dripping off the tip. Occasionally, blockage of the needle or nozzle occurs as a result of the solvent rapidly evaporating, solidifying the droplet inside the needle or nozzle [74,75].

5.5. Collecting Distance

In the sense that the collecting distance is proportional to the electric field intensity, the solution traveling time can be directly influenced. In some cases, shorter collecting distances can be advantageous because they apply a stronger electrostatic force to the jet, resulting in a shorter travel time. A stronger electrostatic force can be beneficial because it stretches the jet effectively, resulting in the formation of finer fibers on the collector. However, shorter distances may have the opposite effect, resulting in insufficient solvent evaporation and subsequent formation of wet fiber webs. Similarly, increasing the distance between the jet and the collector can result in a weaker electric field and dripping of the jet halfway to the collector [8,55,73,74].

5.6. Polarity

Electrospinning with a high voltage electrode applied to the nozzle produces a more intense and concentrated electric field on the nozzle, such that when the jet travels the distance between the high charged needle and the collector, it encounters a decreasing electrostatic force. This promotes chaotic whipping instability, which results in a large area of fiber deposition. On the other hand, increasing the collector voltage results in a more intense electric field near the collector, which strengthens the jet movement toward the collector. This effectively eliminates the whipping movement [7].

5.7. Humidity

The morphology of electrospun fibers is affected by ambient humidity, i.e., the interaction of the jet solution and moisture. Humidity has an effect on fiber diameter by altering the rate of solvent evaporation. With increasing humidity, the average diameter of nanofibers decreases. Beaded fibers begin to form in environments with a high relative

Preprints (www.preprints.org) | NOT PEER-REVIEWED | Posted: 27 April 2021 doi:10.20944/preprints202104.0711.v1

humidity. On the other hand, at relatively low humidity levels, the solvent evaporation rate may be high due to the pressure difference between the vapor and ambient air inside the electrospinning chamber. As a result, fibers solidify, resulting in coarser fibers than fibers generated at relatively higher humidity levels [76].

Humidity also has an effect on the surface structure, causing the formation of porous fibers under conditions of rapid evaporation caused by low humidity. This could be attributed to the fact that evaporation removes heat from the jet surface, lowering the surface temperature to a point where tiny ice crystals can form on the filament surface. These microscopic ice crystals are retained until the deposited fibers on the collector's surface exchange heat with the ambient air and reach the ambient temperature [77].

5.8. Temperature

Temperature is assumed to be inextricably linked to polymer properties such as crystallinity and molecular chain orientations [7]. According to Yang et al., as the ambient temperature increases, the surface tension and viscosity of the electrospinning solution decrease. Increased temperature, on the other hand, results in rapid evaporation of the solvent, which can disrupt the electrospinning process. As a result, a balanced temperature point must be established in order to achieve the desired fiber quality [76,78].

6. Common Polymers in Electrospinning

Natural, synthetic, or copolymer polymers can be used in electrospinning, depending on the manufacturer's requirements and material availability. Collagen, chitosan, and fibrinogen are all examples of natural polymers [8]. Due to their immunogenicity and biocompatibility, natural polymers have advantages over synthetic polymers. Collagen and gelatin are natural polymers that can be used as solutions in the electrospinning process. Natural fibers may not suffice in situations where synthetic fibers are readily available. Polyvinyl alcohol (PVA), polyvinylpyrrolidone (PVP), polylactide (PLA), polyglycolide (PGA), poly-D-lactide (PLDA), and polylactide-co-glycolide are a few examples of synthetic polymers (PLGA) [57]. Copolymers can be created by combining natural or synthetic fibers or by combining several synthetic fibers [60].

The objective is to develop polymers that are resistant to a variety of constraints, including heat and degradation. Copolymers are frequently created to overcome the inherent limitations of a particular natural or synthetic polymer [61]. For instance, poly (glycolide) can be added to poly (ethylene-co-vinyl alcohol) to reduce its stiffness or rigidity (PEVA) [62]. The majority of copolymers exhibit a variety of properties that manufacturers require in order to develop suitable nanofibers.

7. Promising Applications of Ultra-fine Fibers via Electrospinning

Electrospun fibers can be nanoscale in size and have nanoscale surface texture, resulting in a variety of modes of interaction when compared to macroscale materials. Electrospun ultra-fine fibers exhibit two significant properties: a high surface-to-volume ratio and a relatively defect-free molecular structure. Due to the high surface to volume ratio, electrospun materials are well suited for activities requiring increased physical contact, such as providing a site for a chemical reaction or filtration of small-sized physical materials. Additionally, minimal molecular defects enable electrospun fibers to achieve maximum strength, resulting in high mechanical performance for composite materials [79].

There are numerous applications where electrospun fiber can act as a filter; for example, the Lycopodium moss spores have a diameter of 60 micrometers and thus can be captured only by electrospun polyvinyl alcohol fiber. Nanofiber webs may be an effective filtering medium due to the nanofibers' low London-Van Der Waals forces, which are required for the fibers to adhere to one another. In textile manufacturing, nanofibers enable the development of seamless nonwoven garments with a range of functions, including environmental, flame, and chemical protection. Electrospinning enables the combination of

Preprints (www.preprints.org) | NOT PEER-REVIEWED | Posted: 27 April 2021 doi:10.20944/preprints202104.0711.v1

multiple coatings and fibers to create three-dimensional shapes, such as clothing composed of multiple polymer layers [80].

The medical application of nanofibers entails tissue engineering, in which an electrospun scaffold is penetrated by cells that treat or replace biological targets [81]. Additionally, wound dressings made of nanofibers excel at isolating the wound from microbial infections [82]. Electrospinning plays a critical role in the development of medical textile materials and a variety of fibrous treatment delivery systems such as transdermal patches and implants. Electrospinning has the potential to enable the pharmaceutical industry to establish a continuous manufacturing system. Electrospinning is a method for converting synthesized liquids into tablets [83][84][85][86][87][88][89].

Electrospinning is a viable process capable of producing elongated composite materials within a specified timeframe. The process has the potential to produce sufficient fibers in a reasonable amount of time. Electrospinning has been shown to be the most cost-effective method of manufacturing a variety of medical fibers such as medical implants, scaffolds, and wound dressings for artificial human tissues. Scaffolds behave similarly to the extracellular matrix that exists in natural tissues [90][91][92][93]. Biodegradable fibers serve as an extracellular matrix and can be coated with collages to aid in cell attachment. The final application of electrospun fibers is as catalysts, serving as a surface on which enzymes can be immobilized. The enzyme may be critical in the decomposition of toxic chemicals found in the environment [94]. Electrospinning is used to create fibers for energy conversion and storage. Electrospinning produces fibers ranging in diameter from nanometers to micrometers [95]. Fibers not only provide adequate storage space, but also play a critical role in converting stored energy to electrical currents. A standard spinning setup includes a high-voltage power supply, a grounded collector, and a syringe fitted with a metallic needle [96]. Ultra-fine fibers resulted from electrospinning exhibit two significant properties: a high surface-to-volume ratio and a relatively defect-free molecular structure. Due to the high surface to volume ratio of ultra-fine textiles (as seen in 8), electrospun materials are well suited for activities requiring increased physical contact, such as providing a site for a chemical reaction or filtration of small-sized physical materials within a Li-ion battery [59][97].

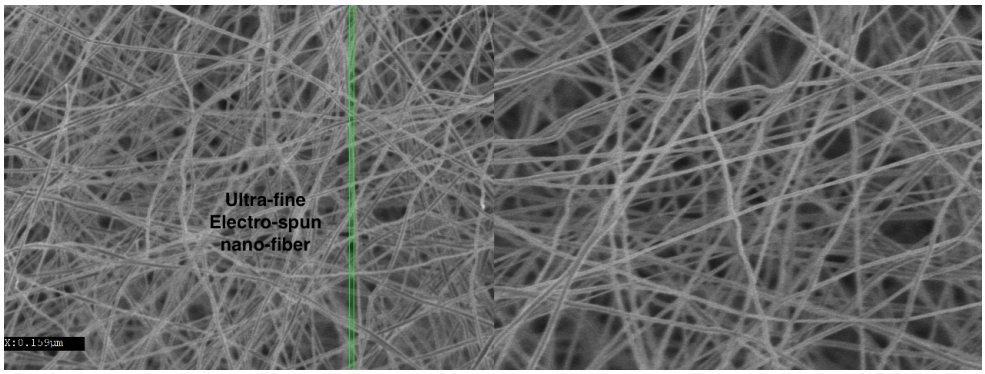

Figure 8. An example of uniform ultra-fine nano-fibers (diameter < ∼150 nm) resulted from polymerized electro-spun V_2O_5/GO tailored for Li-ion cathode materials suitable for the fabrication of ultra-high capacity Li-ion batteries [59]

In most cases, the voltage is supplied via a melt or a solution. As the syringe is heated further, a pendant droplet forms beneath it. Electrostatic repulsion is used to transform the pendant droplet into a cone-shaped material called a Taylor cone. The conical droplet discharges polymer solution at the needle's tip as the electrostatic propulsion continues [98]. The electric field's interaction with the surface tension eventually causes the solvent to evaporate, leaving a long, thin filament that solidifies into a uniform fiber. Electrospinning began in the 1930s, and experts have since used it to develop fibers for energy storage and

 doi:10.20944/preprints202104.0711.v1

conversion within lithium-ion batteries [99]. Numerous modifications have been made to the process to make it more energy efficient and productive.

Electrospinning has a number of advantages, including its ability to operate at a range of temperatures, a short production cycle, and low pressure. Additionally, hydrothermally synthesized nanofibers have a lower aspect ratio, which is critical for energy transfer [100]. In other words, electrospun fibers are likely to be more efficient at transferring energy than other methods, such as electrospun nanowovens [101]. However, electrospinning has a number of limitations, including difficulty producing inorganic nanofibers and a limited number or variety of polymers used in the process. Due to the scarcity of polymers, manufacturers are forced to use materials that may not achieve the desired energy capacities [102]. Additionally, the performance of nanofibers synthesized from inorganic materials is likely to degrade following calcination. Additionally, manufacturers remain silent about the aging process that degrades the efficiency of many batteries. The aging process depletes the energy capacity of various cells and degrades lithium-ion battery performance. There is ongoing research to ascertain the cause of aging and to develop appropriate interventions [103].

8. Conclusion

Electrospun ultra-fine fibers exhibit two significant properties: a high surface-to-volume ratio and a relatively defect-free molecular structure. Due to the high surface to volume ratio, electrospun materials are well suited for activities requiring increased physical contact, such as providing a site for a chemical reaction or filtration of small-sized physical materials. Additionally, minimal molecular defects enable electrospun fibers to achieve maximum strength, resulting in high mechanical performance for composite materials.

Electrospinning yields fibers ranging in diameter from nanometers to micrometers.The fibers not only provide adequate storage space, but also play a critical role in converting the stored energy to electrical currents. Electrospinning has a number of advantages, including its ability to operate at a range of temperatures, a short manufacturing cycle, and low pressure. Additionally, the hydrothermal method produces nanofibers with a lower aspect ratio, which is critical for energy transfer. In other words, electrospun fibers are likely to be more efficient at transferring energy than other methods, such as electrospun nanowovens. Electrospinning, on the other hand, has a number of limitations, including difficulties in preparing inorganic nanofibers and a limited quantity or variety of polymers used in the process. Due to the limited variety of polymers available, manufacturers are forced to use materials that may not achieve the desired energy capacities. Additionally, the performance of nanofibers synthesized from inorganic materials is likely to degrade following calcination. Additionally, manufacturers remain silent about the aging process that degrades the efficiency of many batteries. The aging process depletes the energy capacity of various cells and degrades lithium-ion battery performance.

Conflicts of Interest: The authors declare no conflict of interest.

References

1. Subbiah, T.; Bhat, G.; Tock, R.; Parameswaran, S.; Ramkumar, S. Electrospinning of nanofibers. *Journal of applied polymer science* **2005**, *96*, 557–569.
2. Anton, F. Process and apparatus for preparing artificial threads, 1934. US Patent 1,975,504.
3. D'Avino, G.; Muccioli, L.; Castet, F.; Poelking, C.; Andrienko, D.; Soos, Z.G.; Cornil, J.; Beljonne, D. Electrostatic phenomena in organic semiconductors: fundamentals and implications for photovoltaics. *Journal of Physics: Condensed Matter* **2016**, *28*, 433002.
4. Xiao, K.; Zhou, Y.; Kong, X.Y.; Xie, G.; Li, P.; Zhang, Z.; Wen, L.; Jiang, L. Electrostatic-charge-and electric-field-induced smart gating for water transportation. *ACS nano* **2016**, *10*, 9703–9709.
5. Hughes, J.; Schaub, H. Effects of charged dielectrics on electrostatic force and torque. International Workshop on Spacecraft Formation Flying, 2017.

6. Bhardwaj, N.; Kundu, S.C. Electrospinning: a fascinating fiber fabrication technique. *Biotechnology advances* **2010**, *28*, 325–347.
7. Lin, T.; Fang, J. *Fundamentals of electrospinning and electrospun nanofibers*; DEStech Publications, 2017.
8. Angammana, C.J.; Jayaram, S.H. Fundamentals of electrospinning and processing technologies. *Particulate Science and Technology* **2016**, *34*, 72–82.
9. Li, D.; Xia, Y. Electrospinning of nanofibers: reinventing the wheel? *Advanced materials* **2004**, *16*, 1151–1170.
10. Greiner, A.; Wendorff, J.H. Electrospinning: a fascinating method for the preparation of ultrathin fibers. *Angewandte Chemie International Edition* **2007**, *46*, 5670–5703.
11. Luo, C.; Stoyanov, S.D.; Stride, E.; Pelan, E.; Edirisinghe, M. Electrospinning versus fibre production methods: from specifics to technological convergence. *Chemical Society Reviews* **2012**, *41*, 4708–4735.
12. Sill, T.J.; von Recum, H.A. Electrospinning: applications in drug delivery and tissue engineering. *Biomaterials* **2008**, *29*, 1989–2006.
13. Harfenist, S.A.; Cambron, S.D.; Nelson, E.W.; Berry, S.M.; Isham, A.W.; Crain, M.M.; Walsh, K.M.; Keynton, R.S.; Cohn, R.W. Direct drawing of suspended filamentary micro-and nanostructures from liquid polymers. *Nano Letters* **2004**, *4*, 1931–1937.
14. Ondarcuhu, T.; Joachim, C. Drawing a single nanofibre over hundreds of microns. *EPL (Europhysics Letters)* **1998**, *42*, 215.
15. Xing, X.; Wang, Y.; Li, B. Nanofiber drawing and nanodevice assembly in poly (trimethylene terephthalate). *Optics express* **2008**, *16*, 10815–10822.
16. Tokarev, A.; Trotsenko, O.; Griffiths, I.M.; Stone, H.A.; Minko, S. Magnetospinning of Nano-and Microfibers. *Advanced Materials* **2015**, *27*, 3560–3565.
17. Baumgartner, R.; Eitzlmayr, A.; Matsko, N.; Tetyczka, C.; Khinast, J.; Roblegg, E. Nano-extrusion: a promising tool for continuous manufacturing of solid nano-formulations. *International journal of pharmaceutics* **2014**, *477*, 1–11.
18. Khinast, J.; Baumgartner, R.; Roblegg, E. Nano-extrusion: a one-step process for manufacturing of solid nanoparticle formulations directly from the liquid phase. *AAPS PharmSciTech* **2013**, *14*, 601–604.
19. Bo, Z. Production of polypropylene melt blown nonwoven fabrics: Part II—Effect of process parameters **2012**.
20. Grimm, S.; Giesa, R.; Sklarek, K.; Langner, A.; Gosele, U.; Schmidt, H.W.; Steinhart, M. Nondestructive replication of self-ordered nanoporous alumina membranes via cross-linked polyacrylate nanofiber arrays. *Nano letters* **2008**, *8*, 1954–1959.
21. Dang, X.; Yi, H.; Ham, M.H.; Qi, J.; Yun, D.S.; Ladewski, R.; Strano, M.S.; Hammond, P.T.; Belcher, A.M. Virus-templated self-assembled single-walled carbon nanotubes for highly efficient electron collection in photovoltaic devices. *Nature Nanotechnology* **2011**, *6*, 377.
22. Jun, H.; Yuwono, V.; Paramonov, S.E.; Hartgerink, J.D. Enzyme-mediated degradation of peptide-amphiphile nanofiber networks. *Advanced Materials* **2005**, *17*, 2612–2617.
23. Haynes, C.L.; Van Duyne, R.P. Nanosphere lithography: a versatile nanofabrication tool for studies of size-dependent nanoparticle optics, 2001.
24. Pisignano, D.; Maruccio, G.; Mele, E.; Persano, L.; Di Benedetto, F.; Cingolani, R. Polymer nanofibers by soft lithography. *Applied Physics Letters* **2005**, *87*, 123109.
25. Dabirian, F.; Ravandi, S.H.; Pishevar, A.; Abuzade, R. A comparative study of jet formation and nanofiber alignment in electrospinning and electrocentrifugal spinning systems. *Journal of Electrostatics* **2011**, *69*, 540–546.
26. Sarkar, K.; Gomez, C.; Zambrano, S.; Ramirez, M.; de Hoyos, E.; Vasquez, H.; Lozano, K. Electrospinning to forcespinning^{TM}. *Materials Today* **2010**, *13*, 12–14.
27. Nagaraju, G.; Tharamani, C.; Chandrappa, G.; Livage, J. Hydrothermal synthesis of amorphous MoS 2 nanofiber bundles via acidification of ammonium heptamolybdate tetrahydrate. *Nanoscale research letters* **2007**, *2*, 461.
28. Gorrasi, G.; Sorrentino, A. Mechanical milling as a technology to produce structural and functional bio-nanocomposites. *Green Chemistry* **2015**, *17*, 2610–2625.
29. Badrossamay, M.R.; McIlwee, H.A.; Goss, J.A.; Parker, K.K. Nanofiber assembly by rotary jet-spinning. *Nano letters* **2010**, *10*, 2257–2261.
30. Bronikowski, M.J. CVD growth of carbon nanotube bundle arrays. *Carbon* **2006**, *44*, 2822–2832.
31. Shi, X.; Zhou, W.; Ma, D.; Ma, Q.; Bridges, D.; Ma, Y.; Hu, A. Electrospinning of nanofibers and their applications for energy devices. *Journal of Nanomaterials* **2015**, *16*, 122.

32. Neves, N.M. *Electrospinning for Advanced Biomedical Applications and Therapies*; Smithers Rapra, 2012.
33. Leach, M.K.; Feng, Z.Q.; Tuck, S.J.; Corey, J.M. Electrospinning fundamentals: optimizing solution and apparatus parameters. *JoVE (Journal of Visualized Experiments)* **2011**, p. e2494.
34. Agarwal, S.; Wendorff, J.H.; Greiner, A. Use of electrospinning technique for biomedical applications. *Polymer* **2008**, *49*, 5603–5621.
35. Li, W.; Tuan, R.S. Fabrication and application of nanofibrous scaffolds in tissue engineering. *Current protocols in cell biology* **2009**, *42*, 25.2. 1–25.2. 12.
36. Brown, T.D.; Dalton, P.D.; Hutmacher, D.W. Melt electrospinning today: An opportune time for an emerging polymer process. *Progress in Polymer Science* **2016**, *56*, 116–166.
37. Yousefzadeh, M., Modeling and simulation of the electrospinning process. In *Electrospun Nanofibers*; Elsevier, 2017; pp. 277–301.
38. Ali, U.; Niu, H.; Abbas, A.; Shao, H.; Lin, T. Online stretching of directly electrospun nanofiber yarns. *RSC advances* **2016**, *6*, 30564–30569.
39. Ahmadian, A. Design and Fabrication of High Capacity Lithium-Ion Batteries using Electro-Spun Graphene Modified Vanadium Pentoxide Cathodes. PhD thesis, 2019.
40. Shuakat, M.N.; Lin, T. Recent developments in electrospinning of nanofiber yarns. *Journal of nanoscience and nanotechnology* **2014**, *14*, 1389–1408.
41. Démuth, B.; Farkas, A.; Pataki, H.; Balogh, A.; Szabó, B.; Borbás, E.; Sóti, P.L.; Vigh, T.; Kiserdei, ; Farkas, B. Detailed stability investigation of amorphous solid dispersions prepared by single-needle and high speed electrospinning. *International journal of pharmaceutics* **2016**, *498*, 234–244.
42. Susanto, H.; Samsudin, A.; Faz, M.; Rani, M. Impact of post-treatment on the characteristics of electrospun poly (vinyl alcohol)/chitosan nanofibers. AIP Conference Proceedings. AIP Publishing, Vol. 1725, p. 020087.
43. Zhou, F.; Gong, R.; Porat, I. Mass production of nanofibre assemblies by electrostatic spinning. *Polymer International* **2009**, *58*, 331–342.
44. Wang, X.; Niu, H.; Lin, T.; Wang, X. Needleless electrospinning of nanofibers with a conical wire coil. *Polymer Engineering Science* **2009**, *49*, 1582–1586.
45. Cosio, M.S.; Benedetti, S.; Scampicchio, M.; Mannino, S., Electroanalysis in food process control. In *Agricultural and food electroanalysis*; John Wiley Sons, Ltd Chichester, UK, 2015; pp. 421–441.
46. Yarin, A.L.; Koombhongse, S.; Reneker, D.H. Taylor cone and jetting from liquid droplets in electrospinning of nanofibers. *Journal of applied physics* **2001**, *90*, 4836–4846.
47. Guo, H.F.; Xu, B.G. Numerical study of Taylor cone dynamics in electrospinning of nanofibers. Key Engineering Materials. Trans Tech Publ, Vol. 730, pp. 510–515.
48. Guerrero, J.; Rivero, J.; Gundabala, V.R.; Perez-Saborid, M.; Fernandez-Nieves, A. Whipping of electrified liquid jets. *Proceedings of the National Academy of Sciences* **2014**, *111*, 13763–13767.
49. Sadeghi, D.; Karbasi, S.; Razavi, S.; Mohammadi, S.; Shokrgozar, M.A.; Bonakdar, S. Electrospun poly (hydroxybutyrate)/chitosan blend fibrous scaffolds for cartilage tissue engineering. *Journal of Applied Polymer Science* **2016**, *133*.
50. Aliheidari, N.; Ameli, A.; Potschke, P. Solvent sensitivity of smart 3D-printed nanocomposite liquid sensor. Behavior and Mechanics of Multifunctional Materials and Composites XII. International Society for Optics and Photonics, Vol. 10596, p. 105960V.
51. Hansen, C.M. *Hansen solubility parameters: a user's handbook*; CRC press, 2002.
52. Huang, Z.M.; Zhang, Y.Z.; Kotaki, M.; Ramakrishna, S. A review on polymer nanofibers by electrospinning and their applications in nanocomposites. *Composites science and technology* **2003**, *63*, 2223–2253.
53. Jirsak, O.; Sanetrnik, F.; Lukas, D.; Kotek, V.; Martinova, L.; Chaloupek, J. Method of nanofibres production from a polymer solution using electrostatic spinning and a device for carrying out the method, 2009. US Patent 7,585,437.
54. Luzio, A.; Canesi, E.; Bertarelli, C.; Caironi, M. Electrospun polymer fibers for electronic applications. *Materials* **2014**, *7*, 906–947.
55. Khajavi, R.; Abbasipour, M., Controlling nanofiber morphology by the electrospinning process. In *Electrospun Nanofibers*; Elsevier, 2017; pp. 109–123.
56. Erdem, R.; Usta, I.; Akalin, M.; Atak, O.; Yuksek, M.; Pars, A. The impact of solvent type and mixing ratios of solvents on the properties of polyurethane based electrospun nanofibers. *Applied Surface Science* **2015**, *334*, 227–230.
57. Lin, T.; Wang, H.; Wang, H.; Wang, X. Effects of polymer concentration and cationic surfactant on the morphology of electrospun polyacrylonitrile nanofibres. *Journal of materials science technology* **2005**, *21*, 1–4.

58. Bercea, M.; Morariu, S.; Ioan, C.; Ioan, S.; Simionescu, B.C. Viscometric study of extremely dilute polyacrylonitrile solutions. *European polymer journal* **1999**, *35*, 2019–2024.
59. Ahmadian, A. Design and fabrication of high capacity lithium-ion batteries using electro-spun graphene modified vanadium pentoxide cathodes. PhD thesis, Purdue University Graduate School, 2020.
60. Gupta, P.; Elkins, C.; Long, T.E.; Wilkes, G.L. Electrospinning of linear homopolymers of poly (methyl methacrylate): exploring relationships between fiber formation, viscosity, molecular weight and concentration in a good solvent. *Polymer* **2005**, *46*, 4799–4810.
61. Shenoy, S.L.; Bates, W.D.; Frisch, H.L.; Wnek, G.E. Role of chain entanglements on fiber formation during electrospinning of polymer solutions: good solvent, non-specific polymer–polymer interaction limit. *Polymer* **2005**, *46*, 3372–3384.
62. Shenoy, S.L.; Bates, W.D.; Wnek, G. Correlations between electrospinnability and physical gelation. *Polymer* **2005**, *46*, 8990–9004.
63. Moriya, A.; Shen, P.; Ohmukai, Y.; Maruyama, T.; Matsuyama, H. Reduction of fouling on poly (lactic acid) hollow fiber membranes by blending with poly (lactic acid)–polyethylene glycol–poly (lactic acid) triblock copolymers. *Journal of membrane science* **2012**, *415*, 712–717.
64. Estanqueiro, M.; Vasconcelos, H.; Lobo, J.M.S.; Amaral, H., Delivering miRNA modulators for cancer treatment. In *Drug Targeting and Stimuli Sensitive Drug Delivery Systems*; Elsevier, 2018; pp. 517–565.
65. Hsu, C.M.; Shivkumar, S. Nano-sized beads and porous fiber constructs of poly (-caprolactone) produced by electrospinning. *Journal of Materials Science* **2004**, *39*, 3003–3013.
66. Wu, Y.K.; Wang, L.; Fan, J.; Shou, W.; Zhou, B.M.; Liu, Y. Multi-jet electrospinning with auxiliary electrode: The influence of solution properties. *Polymers* **2018**, *10*, 572.
67. Li, X.; Lin, J.; Zeng, Y. Electric field distribution and initial jet motion induced by spinneret configuration for molecular orientation in electrospun fibers. *European Polymer Journal* **2018**, *98*, 330–336.
68. Meechaisue, C.; Dubin, R.; Supaphol, P.; Hoven, V.P.; Kohn, J. Electrospun mat of tyrosine-derived polycarbonate fibers for potential use as tissue scaffolding material. *Journal of Biomaterials Science, Polymer Edition* **2006**, *17*, 1039–1056.
69. Balogh, A.; Cselkó, R.; Démuth, B.; Verreck, G.; Mensch, J.; Marosi, G.; Nagy, Z.K. Alternating current electrospinning for preparation of fibrous drug delivery systems. *International journal of pharmaceutics* **2015**, *495*, 75–80.
70. Balogh, A.; Farkas, B.; Pálvölgyi, ; Domokos, A.; Démuth, B.; Marosi, G.; Nagy, Z.K. Novel alternating current electrospinning of hydroxypropylmethylcellulose acetate succinate (HPMCAS) nanofibers for dissolution enhancement: The importance of solution conductivity. *Journal of pharmaceutical sciences* **2017**, *106*, 1634–1643.
71. Pokorny, P.; Kostakova, E.; Sanetrnik, F.; Mikes, P.; Chvojka, J.; Kalous, T.; Bilek, M.; Pejchar, K.; Valtera, J.; Lukas, D. Effective AC needleless and collectorless electrospinning for yarn production. *Physical Chemistry Chemical Physics* **2014**, *16*, 26816–26822.
72. Kessick, R.; Fenn, J.; Tepper, G. The use of AC potentials in electrospraying and electrospinning processes. *Polymer* **2004**, *45*, 2981–2984.
73. Theron, S.; Zussman, E.; Yarin, A. Experimental investigation of the governing parameters in the electrospinning of polymer solutions. *Polymer* **2004**, *45*, 2017–2030.
74. Srivastava, R., Electrospinning of patterned and 3D nanofibers. In *Electrospun Nanofibers*; Elsevier, 2017; pp. 399–447.
75. Wang, L.; Ryan, A., Introduction to electrospinning. In *Electrospinning for tissue regeneration*; Elsevier, 2011; pp. 3–33.
76. De Vrieze, S.; Van Camp, T.; Nelvig, A.; Hagström, B.; Westbroek, P.; De Clerck, K. The effect of temperature and humidity on electrospinning. *Journal of materials science* **2009**, *44*, 1357–1362.
77. Pelipenko, J.; Kristl, J.; Janković, B.; Baumgartner, S.; Kocbek, P. The impact of relative humidity during electrospinning on the morphology and mechanical properties of nanofibers. *International journal of pharmaceutics* **2013**, *456*, 125–134.
78. Yang, G.Z.; Li, H.P.; Yang, J.H.; Wan, J.; Yu, D.G. Influence of working temperature on the formation of electrospun polymer nanofibers. *Nanoscale research letters* **2017**, *12*, 55.
79. An, Q.; Li, Y.; Yoo, H.D.; Chen, S.; Ru, Q.; Mai, L.; Yao, Y. Graphene decorated vanadium oxide nanowire aerogel for long-cycle-life magnesium battery cathodes. *Nano Energy* **2015**, *18*, 265–272.
80. Barbosa, G.d.N.; Graeff, C.F.d.O.; Oliveira, H.P. Thermal annealing effects on vanadium pentoxide xerogel films. *Eclética Química* **2005**, *30*, 7–15.

81. Daemi, N.; Ahmadian, A.; Mirbagheri, A.; Ahmadian, A.; Saberi, H.; Amidi, F.; Alirezaie, J. Planning screw insertion trajectory in lumbar spinal fusion using pre-operative CT images. 2015 37th Annual International Conference of the IEEE Engineering in Medicine and Biology Society (EMBC). IEEE, 2015, pp. 3639–3642.
82. Monyoncho, E.A.; Bissessur, R.; Dahn, D.C.; Trenton, V. Intercalation of poly [oligo (ethylene glycol) oxalate] into vanadium pentoxide xerogel. *Alkali-ion batteries* **2016**, pp. 93–110.
83. Reina, G.; González-Domínguez, J.M.; Criado, A.; Vázquez, E.; Bianco, A.; Prato, M. Promises, facts and challenges for graphene in biomedical applications. *Chemical Society Reviews* **2017**, *46*, 4400–4416.
84. Shafiee, A.; Ahmadian, M.T.; Hoursan, H.; Hoviat Talab, M. Effect of linear and rotational acceleration on human brain. *Modares Mechanical Engineering* **2015**, *15*, 248–260.
85. Shafiee, A.; Ahmadian, M.T.; Hoviattalab, M. Mechanical characterization of brain tissue in compression. International Design Engineering Technical Conferences and Computers and Information in Engineering Conference. American Society of Mechanical Engineers, 2016, Vol. 50138, p. V003T11A001.
86. Shafiee, A.; Ahmadian, M.T.; Hoviattalab, M. Traumatic Brain Injury Caused by+ Gz Acceleration. ASME 2016 International Design Engineering Technical Conferences and Computers and Information in Engineering Conference. American Society of Mechanical Engineers Digital Collection, 2016.
87. Khezrloo, A.; Tayebi, M.; Shafiee, A.; Aghaie, A. Evaluation of compressive and split tensile strength of slag based aluminosilicate geopolymer reinforced by waste polymeric materials using Taguchi method. *Materials Research Express* **2021**, *8*, 025504.
88. Jiang, F.; Roberts, W.E.; Liu, Y.; Shafiee, A.; Chen, J. Mechanical environment for lower canine T-loop retraction compared to en-masse space closure with a power-arm attached to either the canine bracket or the archwire. *The Angle Orthodontist* **2020**, *90*, 801–810.
89. Shafiee, A.; Mosadegh, P.; Bashash, S.; Jalili, N. Study of Cross-coupling Effect in Piezo-flexural Nanopositioning Stages. *Modares Mechanical Engineering* **2014**, *14*, 1–8.
90. Poudel, B.K.; Doh, K.O.; Byeon, J.H. Green and continuous route to assemble lateral nanodimensional graphitic oxide composites without process interruption. *Green Chemistry* **2018**, *20*, 2984–2989.
91. Akbar, M.; Ahmadian, A.; Sadeghi, M.J.; Ahmadian, A.; Farahmand, F.; Sarkar, S.; others. Robotic guide for brain biopsy, 2020. US Patent 10,555,784.
92. Ahmadian, A.; Sadeghi, M.J.; Ahmadian, A.; Farahmand, F.; Sarkar, S.; others. Device for brain biopsy, 2018. US Patent App. 15/854,442.
93. Ahmadian, A. A Review on Recent Selective Laser Sintering Printing of Medicines. Technical report, EasyChair, 2021.
94. Korkmaz, S.; Tezel, F.M.; Kariper, I. Synthesis and Characterization of GO/V2O5 Thin Film Supercapacitor. *Synthetic Metals* **2018**, *242*, 37–48.
95. Abdollahi, H.; Samkan, M.; Hashemi, M.M. Facile and fast electrospinning of crystalline ZnO 3D interconnected nanoporous nanofibers for ammonia sensing application. *Microsystem Technologies* **2018**, *24*, 3741–3749.
96. Park, Y.; Lim, H.; Moon, J.H.; Lee, H.N.; Son, S.; Kim, H.; Kim, H.J. High-yield one-pot recovery and characterization of nanostructured cobalt oxalate from spent lithium-ion batteries and successive re-synthesis of LiCoO2. *Metals* **2017**, *7*, 303.
97. Aliahmad, N.; Liu, Y.; Xie, J.; Agarwal, M. V2O5/graphene hybrid supported on paper current collectors for flexible ultrahigh-capacity electrodes for lithium-ion batteries. *ACS applied materials & interfaces* **2018**, *10*, 16490–16499.
98. Singh, L.; Kumar, A.; Lee, H.; Lee, J.; Ji, M.; Lee, Y. Ultrafast auto flame synthesis for the mass production of LiCoO 2 as a cathode material for Li-ion batteries. *Journal of Solid State Electrochemistry* **2018**, *22*, 2561–2568.
99. Chiscan, O.; Dumitru, I.; Tura, V.; Stancu, A. PVC/Fe electrospun nanofibers for high frequency applications. *Journal of Materials Science* **2012**, *47*, 2322–2327.
100. Huang, X.; Bahroloomi, D.; Xiao, X. A multilayer composite separator consisting of non-woven mats and ceramic particles for use in lithium ion batteries. *Journal of Solid State Electrochemistry* **2014**, *18*, 133–139.
101. Kumar, R.; Sharma, R.K.; Singh, A.P. Grafted cellulose: a bio-based polymer for durable applications. *Polymer Bulletin* **2018**, *75*, 2213–2242.

 doi:10.20944/preprints202104.0711.v1

102. Shi, C.; Dai, J.; Li, C.; Shen, X.; Peng, L.; Zhang, P.; Wu, D.; Sun, D.; Zhao, J. A modified ceramic-coating separator with high-temperature stability for lithium-ion battery. *Polymers* **2017**, *9*, 159.
103. Zhang, Q.; Tan, S.; Kong, X.; Xiao, Y.; Fu, L. Synthesis of sulfur encapsulated 3D graphene sponge driven by micro-pump and its application in Li–S battery. *Journal of Materiomics* **2015**, *1*, 333–339.

 doi:10.20944/preprints202104.0711.v1